

Calculation of solubility in titanium alloys from first-principles

Roman V. Chepulskii and Stefano Curtarolo[*]

*Department of Mechanical Engineering and Materials Science and
Department of Physics, Duke University, Durham, NC 27708, USA*

(Dated: October 26, 2018)

We present an approach to calculate the atomic bulk solubility in binary alloys based on the statistical-thermodynamic theory of dilute lattice gas. The model considers all the appropriate ground states of the alloy and results in a simple Arrhenius-type temperature dependence determined by a “*low-solubility formation enthalpy*”. This quantity, directly obtainable from first-principle calculations, is defined as the composition derivative of the compound formation enthalpy with respect to nearby ground states. We apply the framework and calculate the solubility of the A specie in A-Ti alloys (A=Ag,Au,Cd,Co,Cr,Ir,W,Zn). In addition to determining unknown low-temperature ground states for the eight alloys, we find qualitative agreements with solubility experimental results. The presented formalism, correct in the low-solubility limit, should be considered as an appropriate starting point for determining if more computationally expensive formalisms are otherwise needed.

PACS numbers:

I. INTRODUCTION

High-throughput *ab initio* methods, capable of predicting properties of an ample set of materials from quantum mechanics calculations, are becoming important tools for scientists working in rational materials development. These methods allow researchers to correlate between different systems and to observe trends converging toward the predictions of new materials [1, 2, 3, 4, 5, 6]. The main difference between the “several-calculations” and the “high-throughput” philosophies is that the latter requires rapid estimations of materials properties so that the correlations between systems, even if roughly characterized, become the target information instead of the throughout and accurate description of a small subset. Clearly, to analyze the extensive amount of information and to extract correlations, ad-hoc algorithms and appropriate computer softwares have to be developed. Furthermore, once the space of the search is narrowed, a detailed study can be employed on the obtained reduced set of feasible candidate systems.

Several examples have appeared in literature in recent years, for instance the “data-mining of quantum calculations” method leading to the principle component analysis of the formation energies of many alloys in several configurations [4, 5], the evolutionary approach for determining hamiltonian [7], the “Pareto-optimal” alloys and catalysts [8, 9] the prediction of the lithium-boron superconductor [10], the “high-throughput Kohn-anomalies” search in ternary lithium-borides [11, 12], and the “multi-optimization” techniques used in studying high-temperature reactions in multicomponent hydrides [13, 14, 15].

This manuscript focuses on the high-throughput formalism for the calculations of solubility in binary alloys (solvus lines). The knowledge of solubility is crucial for designing new alloys with particular physical, chemical,

and mechanical properties. For example, if we have to enhance an alloy property by adding extra specie as solute, it is necessary to know the equilibrium solubility to understand if it is possible to dissolve the candidate specie, and, if possible, to avoid supersaturation-precipitation and subsequent modification of the target property (aging effect). In superconducting materials research, the problem emerges frequently: often expensive and difficult experiments are undertaken to enhance the critical temperature [16, 17]. Even in catalysis research, recent experiments and modeling have shown that the solubility of carbon is responsible of thermodynamic instabilities hindering the catalytic activity of very small Fe and Fe:Mo clusters [18, 19]. The calculation of solubility of Zr in Al has already been addressed with success within the regular solution model [20] fit to *ab initio* calculations [21]. Solubility can also be extracted from the knowledge of the phase diagram which, in the case of lattice-conserving alloys, can be generated within the the cluster expansion [22, 23] and Monte Carlo approaches[24, 25]. However, a straightforward formalism leading to the estimation of equilibrium solubility for general alloys is still lacking.

In the present paper we devised a statistical-thermodynamic approach for the calculation of atomic solubility in alloys. The advantage of our approach consists in taking into account all available ground states rather than just the pure species configurations. To test the method, we present calculations for a number of binary titanium systems. The paper is organized as follows: In Sec. II we rewrite the equations governing solubility in the case of vacancies and substitutional impurities in binary alloys. Section III is devoted to the discussions of capabilities and limits of our formalism. Examples of phase diagrams and solubilities are addressed in Sec. IV for the following test Ti-A systems (A=Ag,Au,Cd,Co,Cr,Ir,W,Zn). Conclusions are given in

Sec. V.

II. SOLUBILITY FORMALISM

Enthalpy

Let us consider a disordered dilute solution of A-atoms and vacancies (V) in a pure B-solid with a given Bravais crystal lattice (labeled with the “*dis*”). Without taking into account the A-A, A-V, and V-V interactions and assuming that A and V concentrations are small, the approximate enthalpy of the considered alloy can be written as:

$$H^{\text{dis}} = E^{\text{dis}} + pV^{\text{dis}} = H_{\text{B}}^{\text{at}}N + H_{\text{AB}}N_{\text{A}} + H_{\text{VB}}N_{\text{V}}, \quad (1)$$

where H_{B}^{at} , H_{AB} and H_{VB} are the enthalpy of the pure B solid per unit cell, the change in enthalpy of the solid upon substitution of one B with an A-atom, and the change in enthalpy upon removal of one B atom, respectively. In addition, N and N_{α} ($\alpha=\text{A,B,V}$) are the total numbers of crystal lattice sites and of atoms of α -type:

$$\begin{aligned} N &= N_{\text{A}} + N_{\text{B}} + N_{\text{V}}, & H_{\text{B}}^{\text{at}} &= E_{\text{B}}^{\text{at}} + pv_{\text{B}}^0, \\ H_{\text{AB}} &= E_{\text{AB}}^0 + pv_{\text{AB}}^0, & H_{\text{VB}} &= E_{\text{VB}}^0 + pv_{\text{VB}}^0, \end{aligned} \quad (2)$$

E_{α}^{at} and v_{α}^0 ($\alpha=\text{A,B}$) are energy and the volume per atom of the α -pure solid, p is the pressure, v_{AB} and v_{VB}^0 represent the change of volume of the B-pure solid upon introduction of one A-atom or one vacancy. The framework introduced by Eq. (1) is similar to Wagner-Schottky model of a system of non-interacting particles.[26]. The quantities with superscript “0” are considered to be temperature, pressure, and composition independent being calculated at zero temperature and pressure. Hence, the accuracy of the following results will be better in the case of limited pressures or for systems with very high bulk modulus, where the elastic energy fraction of E_{α}^{at} is negligible.

The quantities in Eq. (2) can be easily approximated as differences of first-principles energies and volumes between large supercells (sc) with or without defects (substitutional A-atom or vacancy):

$$\begin{aligned} E_{\text{AB}}^0 &\simeq E_{\text{sc}}[B_{n_{\text{sc}}-1}A] - E_{\text{sc}}[B_{n_{\text{sc}}}], \\ v_{\text{AB}}^0 &\simeq V_{\text{sc}}[B_{n_{\text{sc}}-1}A] - V_{\text{sc}}[B_{n_{\text{sc}}}], \\ E_{\text{VB}}^0 &\simeq E_{\text{sc}}[B_{n_{\text{sc}}-1}] - E_{\text{sc}}[B_{n_{\text{sc}}}], \\ v_{\text{VB}}^0 &\simeq V_{\text{sc}}[B_{n_{\text{sc}}-1}] - V_{\text{sc}}[B_{n_{\text{sc}}}]. \end{aligned} \quad (3)$$

As the size of the supercell grows, the approximate quantities in Eqs. (3) approach their exact values. In literature[27] and in this paper, $E_{\alpha\text{B}}^0$, $v_{\alpha\text{B}}^0$ and $H_{\alpha\text{B}}$

($\alpha=\text{A,V}$) are called the “raw” (composition unpreserving) α -defect formation energy, volume and enthalpy, respectively.

The enthalpy per atom is obtained from Eq. (1) as:

$$H_{\text{at}}^{\text{dis}} = H^{\text{dis}}/(N_{\text{A}} + N_{\text{B}}) = \quad (4)$$

$$H_{\text{B}}^{\text{at}} + H_{\text{AB}}x_{\text{A}} + (H_{\text{VB}} + H_{\text{B}}^{\text{at}})x_{\text{V}},$$

where x_{α} ($\alpha=\text{A,B,V}$) are the atomic concentrations

$$x_{\alpha} = N_{\alpha}/(N_{\text{A}} + N_{\text{B}}). \quad (5)$$

Then, we follow the convention of using the *formation* enthalpy $\Delta H_{\text{at}}^{\text{dis}}$ calculated with respect to the pure A- and B-solids [28]:

$$\Delta H_{\text{at}}^{\text{dis}} = H_{\text{at}}^{\text{dis}} - x_{\text{A}}H_{\text{A}}^{\text{at}} - (1 - x_{\text{A}})H_{\text{B}}^{\text{at}}, \quad (6)$$

where $H_{\text{A}}^{\text{at}} = E_{\text{A}}^{\text{at}} + pv_{\text{A}}^0$ and H_{B}^{at} has been defined in Eq. (2). Combining equations (4) and (6), we get

$$\Delta H_{\text{at}}^{\text{dis}} = H_{\text{A}}x_{\text{A}} + H_{\text{V}}x_{\text{V}}, \quad (7)$$

where the quantities H_{A} and H_{V} , defined as

$$H_{\text{A}} = H_{\text{AB}} - H_{\text{A}}^{\text{at}} + H_{\text{B}}^{\text{at}}, \quad H_{\text{V}} = H_{\text{VB}} + H_{\text{B}}^{\text{at}} \quad (8)$$

are usually called A-defect and V-defect “true” (composition preserving)[27] formation enthalpies, which can be obtained from[28]

$$H_{\alpha} = \left. \frac{\partial \Delta H_{\text{at}}^{\text{dis}}}{\partial x_{\alpha}} \right|_{x_{\alpha} \rightarrow 0} \quad (\alpha = \text{A, V}). \quad (9)$$

Equilibrium Gibbs Free Energy

The formation Gibbs free energy, $\Delta G_{\text{at}}^{\text{dis}}$, is defined as:

$$\Delta G_{\text{at}}^{\text{dis}} = \Delta H_{\text{at}}^{\text{dis}} - T\Delta S_{\text{at}}^{\text{dis}}, \quad (10)$$

where $\Delta H_{\text{at}}^{\text{dis}}$ is described by Eq. (7) and the formation entropy $\Delta S_{\text{at}}^{\text{dis}} = S_{\text{at}}^{\text{dis}}$ can be obtained within the mean-field approximation as

$$\Delta S_{\text{at}}^{\text{dis}} = -\frac{k_{\text{B}}N}{N_{\text{A}} + N_{\text{B}}} \sum_{\alpha=\text{A,B,V}} c_{\alpha} \ln c_{\alpha}, \quad (11)$$

where T , k_{B} , c_{α} ($\alpha=\text{A,B,V}$) are the temperature, the Boltzmann constant, and the site concentrations of atoms:

$$c_{\alpha} = N_{\alpha}/N. \quad (12)$$

By changing variables from site concentrations c_{α} to atomic concentrations x_{α} :

$$x_{\alpha} = N_{\alpha}/(N_{\text{A}} + N_{\text{B}}), \quad c_{\alpha} = x_{\alpha}/(1 + x_{\text{V}}), \quad (13)$$

we rewrite Eq. (10) as

$$\Delta G_{\text{at}}^{\text{dis}} = \Delta G_{\text{at}}^{\text{dis,A}} + \Delta G_{\text{at}}^{\text{dis,V}},$$

$$\Delta G_{\text{at}}^{\text{dis,A}} = H_{\text{A}}x_{\text{A}} + k_{\text{B}}T[x_{\text{A}}\ln x_{\text{A}} + (1-x_{\text{A}})\ln(1-x_{\text{A}})],$$

$$\Delta G_{\text{at}}^{\text{dis,V}} = H_{\text{V}}x_{\text{V}} + k_{\text{B}}T[x_{\text{V}}\ln x_{\text{V}} - (1+x_{\text{V}})\ln(1+x_{\text{V}})]. \quad (14)$$

In alloy with fixed atomic composition x_{A} , the equilibrium concentration of vacancies x_{V}^{eq} is determined by minimizing the formation Gibbs free energy:

$$\left. \frac{\partial \Delta G_{\text{at}}^{\text{dis}}}{\partial x_{\text{V}}} \right|_{x_{\text{A}}} = \frac{\partial \Delta G_{\text{at}}^{\text{dis,V}}}{\partial x_{\text{V}}} = 0. \quad (15)$$

The manipulation of Eqs. (14)-(15) leads to:

$$x_{\text{V}}^{\text{eq}} = \left[\exp\left(\frac{H_{\text{V}}}{k_{\text{B}}T}\right) - 1 \right]^{-1},$$

$$x_{\text{V}}^{\text{eq}} \Big|_{k_{\text{B}}T \ll E_{\text{V}}} \simeq \exp\left(-\frac{H_{\text{V}}}{k_{\text{B}}T}\right), \quad (16)$$

$$\Delta G_{\text{at}}^{\text{dis,V}}(x_{\text{V}}^{\text{eq}}) = k_{\text{B}}T \ln \left[1 - \exp\left(-\frac{H_{\text{V}}}{k_{\text{B}}T}\right) \right],$$

$$\Delta G_{\text{at}}^{\text{dis,V}}(x_{\text{V}}^{\text{eq}}) \Big|_{k_{\text{B}}T \ll E_{\text{V}}} \simeq -k_{\text{B}}T \exp\left(-\frac{H_{\text{V}}}{k_{\text{B}}T}\right).$$

To conclude, the ‘‘true’’ vacancies formation enthalpy H_{V} determines the equilibrium concentration of vacancies with an Arrhenius-type equation (see also Ref. 28). In the next section, we show that H_{A} resolves the solubility in the case of a phase-separating alloy having no intermediate ground states.

Solubility

At a given temperature, the solubility of A-atoms in a B-solid phase, $x_{\text{A}_{\text{B}}}^{\text{sol}}$, is defined as the maximum homogeneously achievable concentration of A without the formation of a new phase (Fig. 1(a)). The accurate calculation of $x_{\text{A}_{\text{B}}}^{\text{sol}}$ requires considering of the nearby ground state (labeled as ‘‘gs’’) with respect to the increase of x_{A} , see the ‘‘red line’’ in Fig. 1(b). It is implemented by minimizing the formation Gibbs free energy $\Delta G_{\text{at}}^{\text{mix}}(x)$ of a mixture of (1) a disordered dilute solution of A-atoms and vacancies in a B-rich solid phase at composition $x_{\text{A}_{\text{B}}}$ (the ‘‘dis’’-phase of the previous section), and (2) an on- or off-stoichiometric ground state ‘‘gs’’-phase at composition $x_{\text{A}_{\text{gs}}}$. The lever rule gives the fractions of the two phases:

$$\Delta G_{\text{at}}^{\text{mix}}(x) = \frac{x_{\text{A}_{\text{gs}}}^{-x}}{x_{\text{A}_{\text{gs}}}^{-x} - x_{\text{A}_{\text{B}}}} \Delta G_{\text{at}}^{\text{dis}}(x_{\text{A}_{\text{B}}}) + \frac{x - x_{\text{A}_{\text{B}}}}{x_{\text{A}_{\text{gs}}} - x_{\text{A}_{\text{B}}}} \Delta G_{\text{at}}^{\text{gs}}(x_{\text{A}_{\text{gs}}}), \quad (17)$$

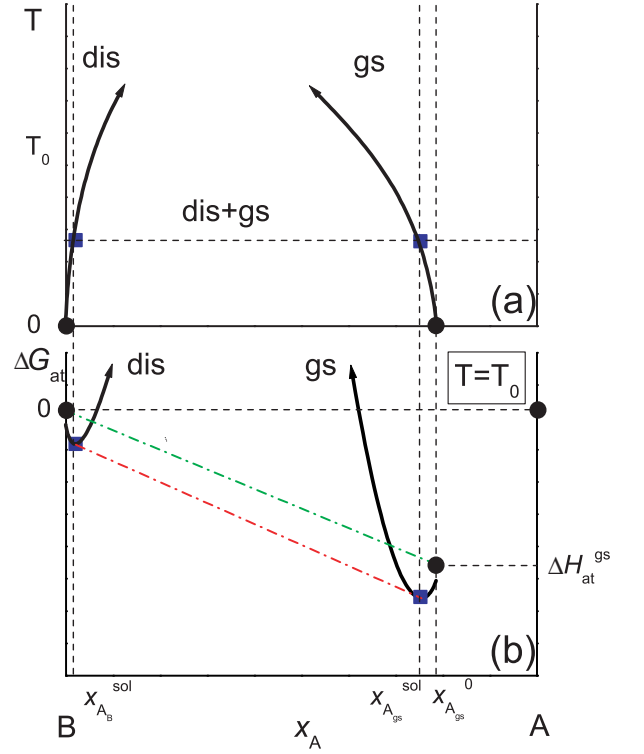


FIG. 1: (Color online) (a) Temperature-concentration and (b) formation Gibbs free energy-concentration (at a given temperature T_0) graphs illustrating our solubility concepts.

and the minimization is performed with respect to $x_{\text{A}_{\text{B}}}$ and $x_{\text{A}_{\text{gs}}}$ (x is the overall composition of A in the two-phase mixture, $x_{\text{A}_{\text{B}}} < x < x_{\text{A}_{\text{gs}}}$):

$$\frac{\partial \Delta G_{\text{at}}^{\text{mix}}}{\partial x_{\text{A}_{\text{B}}}} = 0, \quad \frac{\partial \Delta G_{\text{at}}^{\text{mix}}}{\partial x_{\text{A}_{\text{gs}}}} = 0. \quad (18)$$

Combining Eqs. (17) and (18) leads to the usual *common-tangent* rule:

$$\frac{\partial \Delta G_{\text{at}}^{\text{dis}}(x_{\text{A}_{\text{B}}})}{\partial x_{\text{A}_{\text{B}}}} = \frac{\partial \Delta G_{\text{at}}^{\text{gs}}(x_{\text{A}_{\text{gs}}})}{\partial x_{\text{A}_{\text{gs}}}} = \frac{\Delta G_{\text{at}}^{\text{dis}}(x_{\text{A}_{\text{B}}}) - \Delta G_{\text{at}}^{\text{gs}}(x_{\text{A}_{\text{gs}}})}{x_{\text{A}_{\text{B}}} - x_{\text{A}_{\text{gs}}}}. \quad (19)$$

Substituting Eqs. (14) into Eqs. (19), we obtain

$$x_{\text{A}_{\text{B}}}^{\text{sol}} = [\exp(H_{\text{sol}}/k_{\text{B}}T) + 1]^{-1}, \quad (20)$$

which approximates as an Arrhenius-type relation at low temperature:

$$x_{\text{A}_{\text{B}}}^{\text{sol}} \Big|_{k_{\text{B}}T \ll H_{\text{sol}}} \simeq \exp(-H_{\text{sol}}/k_{\text{B}}T). \quad (21)$$

can be formally determined by minimizing $\Delta G_{\text{at}}^{\text{dis},A}$ (Eq. (14)) with respect to x_A (e.g. Ref. 29). However, in the general case, the existence of ordered ground-states must be verified so the appropriate formalism is used. Generally, in ordering alloys H_A and $H_{\text{sol}}^{1s,nv}$ differ, and might even have different signs.

Note that if the “sc” point is below (B+gs) in Fig. 2 ($H_{\text{sol}}^{1s,nv} < 0$) the solubility expressions (20-21) are not valid, and there must exist an undetected ground state (it might be “sc” itself) with concentration lower than x_{Ags}^0 . In this case, such undetected ground state should be used for the calculation of solubility rather than initial “gs” [30].

The expression for non-binary low-solubility within the regular solution model derived in Refs. [20, 21] coincides with our derivation in the case of binary alloys without vacancies and high-temperature contributions. This is because the regular solution model corresponds to our model for the free energy in case of dilute solution.

IV. GROUND STATES OF SELECTED TITANIUM ALLOYS

As an example of our formalism, we calculate the solubility of a set of metals in titanium. First, we explore the possible ground states of the A-Ti systems (A=Ag,Au,Cd,Co,Cr,Ir,W,Zn) and then we apply the construction described in the previous section.

The low temperature stability of A-Ti is performed by using our high-throughput quantum calculations framework [4, 5, 10, 12], based on first-principles energies obtained with the VASP software [31]. We use projector augmented waves (PAW) pseudopotentials [32] and exchange-correlation functionals as parameterized by Perdew-Burke-Ernzerhof [33] for the generalized gradient approximation (GGA). Simulations are carried out with spin polarization except Ti-Co, at zero temperature and pressure [34], and without zero-point motion. All structures are fully relaxed (shape and volume of the cell and internal positions of the atoms). The effect of lattice vibrations is omitted. Numerical convergence to within about 1 meV/atom is ensured by enforcing a high energy cut-off (357 eV) and dense 6,000 \mathbf{k} -point meshes.

The number of crystal structures considered for the calculations of each A-Ti system is 194. In addition to the 176 described in Ref. 5, we included the following prototypes A5, A6, A7, A11, Ca_7Ge , NbNi_8 (Pt_8Ti), V_4Zn_5 , C36 and the whole complete set of hcp-superstructures with up to 4 atoms/cell. The whole process is performed in an automatic fashion through the software AFLOW which generates the prototypes, optimize the parameters, perform the calculations, correct possible errors, and calculate the phase diagrams [5, 35].

Our results of ground state calculation are presented

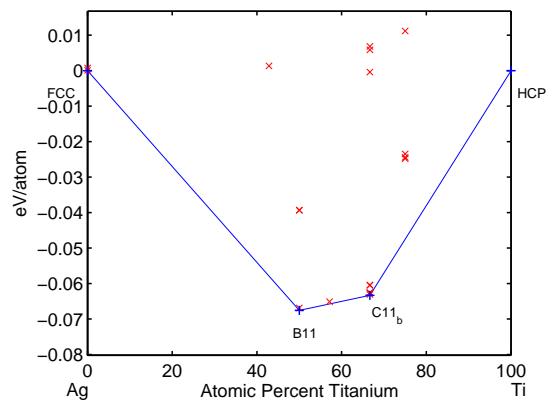


FIG. 3: (Color online) AgTi (silver-titanium) ground state convex hull.

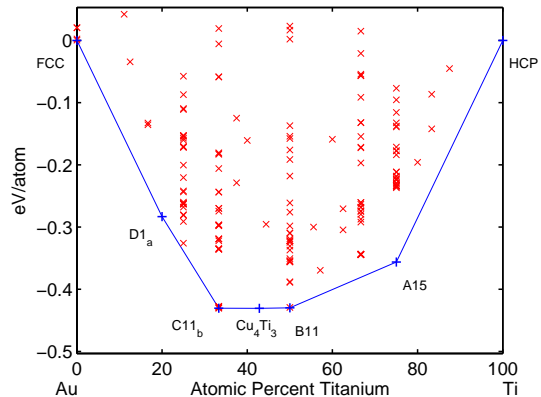


FIG. 4: (Color online) AuTi (gold-titanium) ground state convex hull.

in Figs. 3-10 and Table I. The correspondence *ab initio* versus experimental results is very good and typical for this type of calculations [5].

We propose degenerate results for: 1) Co_2Ti , experimentally reported as C15, but with *ab initio* formation energies of -311.4 meV/at. and -304.0 meV/at. for C14 and C15, respectively; 2) CoTi_2 , experimentally reported

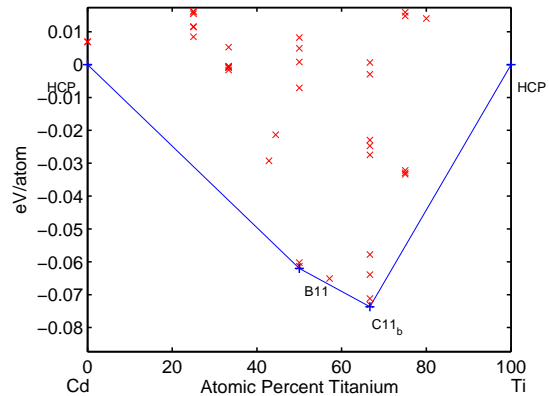


FIG. 5: (Color online) CdTi (cadmium-titanium) ground state convex hull.

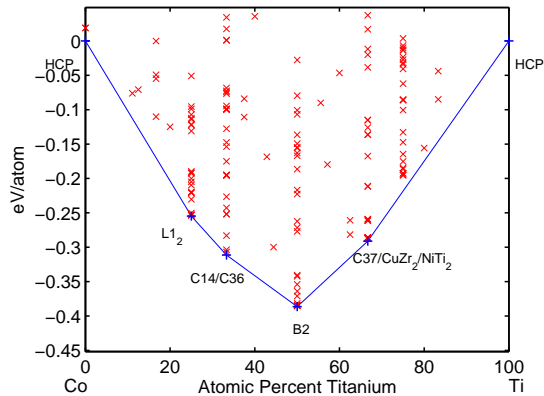


FIG. 6: (Color online) CoTi (cobalt-titanium) ground state convex hull.

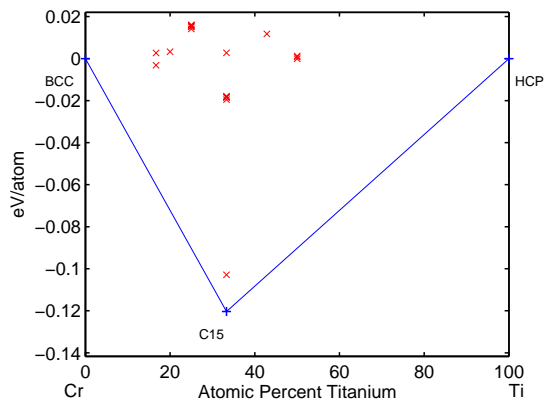


FIG. 7: (Color online) CrTi (chromium-titanium) ground state convex hull.

as NiTi_2 , but with *ab initio* formation energies of -291.2 meV/at., -287.3 meV/at., and -285.7 meV/at. for C37, CuZr_2 , and NiTi_2 , respectively; 3) TiZn , experimentally reported as B2, but with *ab initio* formation energies of -195.4 meV/at. and 193.4 meV/at. for L1_0 and B2, respectively.

We propose the novel results for: 1) Ir_7Ti , experimentally reported as a two phases region above 500°C ,

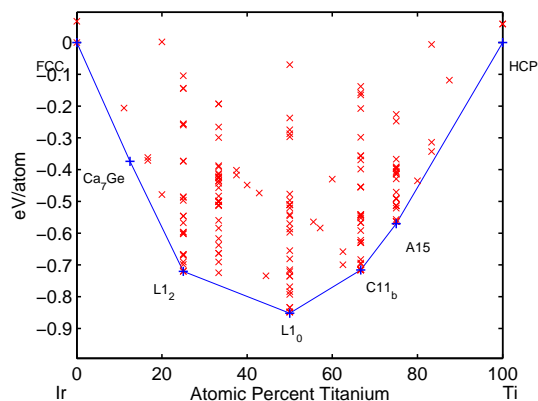


FIG. 8: (Color online) IrTi (iridium-titanium) ground state convex hull.

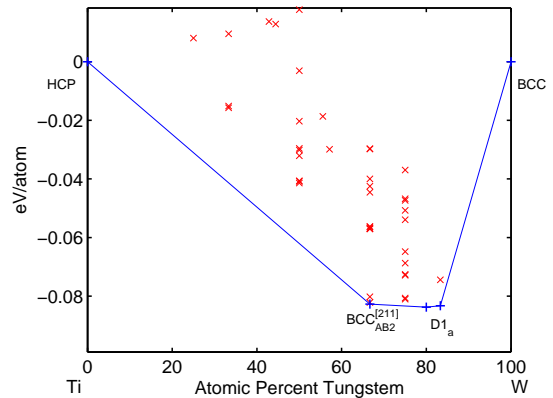


FIG. 9: (Color online) TiW (titanium-tungsten) ground state convex hull.

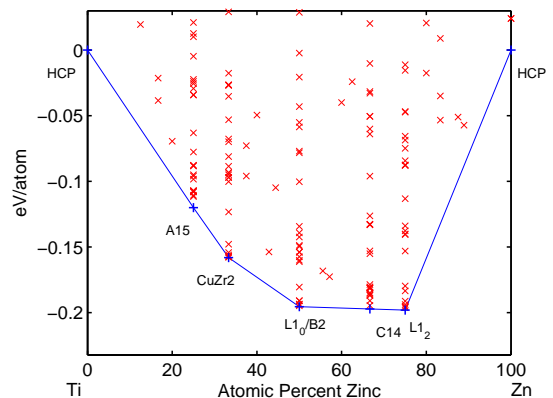


FIG. 10: (Color online) TiZn (titanium-zinc) ground state convex hull.

but with a possible *ab initio* low temperature ground state Ca_7Ge with formation energy of -373.8 meV/at. 2) Ir_2Ti , experimentally reported as a two phases region above 500°C , but with a possible *ab initio* low temperature ground state C11_b , with formation energy of -716.0 meV/at. 3) TiW_2 , experimentally reported as a two phases region above 500°C , but with a possible *ab initio* low temperature ground state $\text{BCC}_{AB2}^{[211]}$, with formation energy of -82.7 meV/at. (see notation for the prototype in Ref. [5]). 4) TiW_4 , experimentally reported as a two phases region above 500°C , but with a possible *ab initio* low temperature ground state D1_a , with formation energy of -83.8 meV/at. 5) Ti_3Zn , experimentally not explored, but with a possible *ab initio* low temperature ground state A15, with formation energy of -120.0 meV/at.

In particular, the results indicate that in the Ir-Ti system the low temperature Ir-rich part of the known phase diagram is not complete, and that the Ti-W alloy has an ordering tendency at low temperature, in contrast to common belief [36, 37]. In addition, in Ti-Zn there must exist a Ti-rich compound with Ti composition higher than the reported Ti_2Zn , [36, 37].

TABLE I: Low temperature phases comparison chart for Ag-Ti, Au-Ti, Cd-Ti, Co-Ti, Cr-Ti, Ir-Ti, Ti-V, and Ti-Zn. Experimental data correspond to the lowest available temperature [5]. The “*” indicates the energy values used in solubility calculations.

Experimental (Refs. 36, 37)	<i>Ab initio</i> result	$\Delta E_{\text{at}}^{\text{gs}}$ (meV/at.)	Space group[38]	Pearson
Ag-Ti				
AgTi-B11	B11	-67.6	P4/nmm	tP4
AgTi ₂ -C11 _b	C11 _b	-63.3*	I4/mmm	tI6
Au-Ti				
Au ₄ Ti-D1 _a	D1 _a	-283.2	I4/m	tI10
Au ₂ Ti-C11 _b	C11 _b	-430.4	I4/mmm	tI6
two-phase region above 500°C	Au ₄ Ti ₃ -Cu ₄ Ti ₃ /tie	-430.6	I4/mmm	tI14
AuTi-B11	B11	-429.8	P4/nmm	tP4
AuTi ₃ -A15	A15	-356.1*	Pm3n	cP8
Cd-Ti				
CdTi-B11	B11	-62.0	P4/nmm	tP4
CdTi ₂ -C11 _b	C11 _b	-73.7*	I4/mmm	tI6
Cr-Ti				
Cr ₂ Ti-C15	C15	-120.3*	Fd3m	cF24
Co-Ti				
Co ₃ Ti-L1 ₂	L1 ₂	-254.8	Pm3m	cP4
Co ₂ Ti-C15	C14	-311.4	P6 ₃ /mm	hP12
	C15	-304.0	Fd3m	cF24
CoTi-B2	B2	-386.4	Pm3m	cP2
CoTi ₂ -NiTi ₂	C37	-291.2*	Pnma	oP12
	CuZr ₂	-287.3	I4/mmm	tI6
	NiTi ₂	-285.7	Fd3m	cF96
Ir-Ti				
two-phase region above 500°C	Ir ₇ Ti-Ca ₇ Ge	-373.8	Fm3m	cF32
Ir ₃ Ti-L1 ₂	L1 ₂	-720.3	Pm3m	cP4
IrTi- δ	L1 ₀	-851.8	P4/mmm	tP4
two-phase region above 500°C	Ir ₂ Ti-C11 _b	-716.0	I4/mmm	tI6
IrTi ₃ -A15	A15/tie	-570.3*	Pm3n	cP8
Ti-W				
two-phase region above 500°C	TiW ₂ -BCC _{AB2} ^[211]	-82.7*	P3m1	hP3
two-phase region above 500°C	TiW ₄ -D1 _a	-83.8	I4/m	tI10
Ti-Zn				
non explored	Ti ₃ Zn-A15	-120.0*	Pm3n	cP8
Ti ₂ Zn-CuZr ₂	CuZr ₂	-158.0	I4/mmm	tI6
TiZn-B2	L1 ₀	-195.4	P4/mmm	tP4
	B2	-193.4	Pm3m	cP2
TiZn ₂ -C14	C14/tie	-197.2	P6 ₃ /mm	hP12
TiZn ₃ -L1 ₂	L1 ₂	-198.0	Pm3m	cP4

V. RESULTS AND DISCUSSION OF SOLUBILITY IN TI ALLOYS

The “raw” formation enthalpies of Ti alloys with one substitutional atom or a vacancy were obtained through Eqs. (3) considering $3 \times 3 \times 3$ supercells of the hcp Ti. Su-

percell dimensions were chosen to limit the defect-defect interactions, being their distance at least three times larger than the nearest neighbor Ti-Ti bond. The results are presented in Table II. Solubilities temperature dependencies are presented in Fig. 11, while Fig. 12 illustrates a comparison of experimental and theoretical data at T=700°C.

TABLE II: “Raw” formation enthalpies H_{ATi} , H_{VTi} (from Eqs. (2-3) at zero pressure), “true” formation enthalpies H_{A} , H_{V} (from Eq. (8) at zero pressure) and low-solubility (non-vacancy) formation enthalpy $H_{\text{sol}}^{\text{ls,nv}}$ (from Eq. (25) at zero pressure) of substitutional A-defects (A=Ag,Au,Cd,Co,Cr) and vacancies (V). The elements are ordered from low to high “low-solubility formation enthalpy”. All quantities are in eV units.

A	H_{ATi}	H_{A}	$H_{\text{sol}}^{\text{ls,nv}}$
Zn	6.405	-0.262	0.218
Cd	7.267	0.24	0.461
Ag	5.412	0.304	0.494
Au	3.882	-0.781	0.643
W	-4.303	0.714	0.838
Ir	-2.059	-1.14	1.141
Co	1.138	0.316	1.19
Cr	-0.674	1.024	1.205
$H_{\text{VTi}} = 10.002, H_{\text{V}} = 2.068$			

Table II shows negative “true” formation enthalpies H_{A} for A=Zn, Au, and Ir. This indicates that calculation of Zn, Au, and Ir solubilities in Ti is not faceable without considering nearby intermetallic ground states.

Figures 11-12 show that the highest theoretical solubilities in Ti occurs for Zn, Cd, Ag, and Au as consequence of their low solubility formation enthalpies (see Table II). This high solubility has also been observed experimentally for Cd, Ag, and Au, whereas, to our best knowledge, solubility of Zn does not seem to have been studied. High solubility of late transition metals Zn, Cd, Ag, and Au in the early transition metal titanium is due to the substantial localized stability provided by the filling tendency of the *d*-band of Ti (Ref. 39).

Because of the very high formation enthalpy of vacancies in Ti (reported in Table II), the vacancy equilibrium concentration was found to be very low at all considered temperatures (e.g. $x_{\text{V}}^{\text{eq}} < 10^{-6}$ at $T < 1300^\circ\text{C}$). Thus, the effect of vacancies on the solubilities of Ti alloys should be negligible.

Although, theoretical and experimental results follow similar trends, theoretical solubilities are considerably smaller for most of the considered alloys. A similar discrepancy was also observed for Al-Zr in Ref. 21. The discrepancy could be due to shortcomings of theory and/or experiment. The main approximations of our model consist of (a) neglecting the defect interaction, (b) neglecting the spatial defect correlation and (c) assuming low concentration of defects. However, as such approxima-

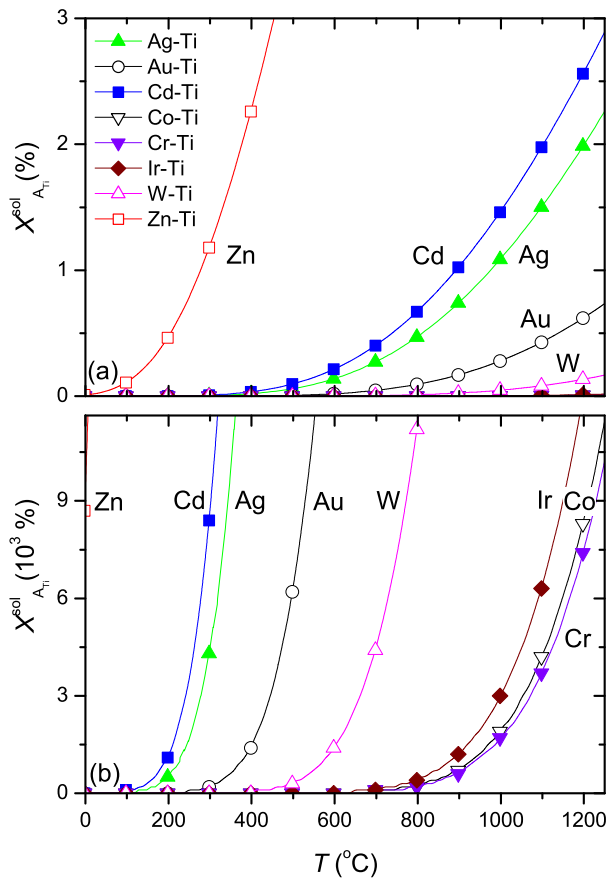


FIG. 11: (Color online) The solubilities of eight considered transition metals in titanium as functions of temperature (calculated through Eqs. (20,24)). Panel (b) is a magnified version of panel (a), to visualize the values for Ir, Co, and Cr.

tions are somehow related, subsequent solubility calculations suggesting low values validate the assumptions (the mean-field approximation neglects the interatomic positional correlations but it should work well when the deviation from complete stoichiometric (pure Ti-solid in our case) is small - and so is the solubility in our case - see Sec. 19 in Ref. 40.) For all considered alloys except Ti-Zn, we found that at intermediate temperatures the calculated solubilities are small enough for our approximations to be valid, although smaller than experiment, as mentioned before. In Ref.21, the authors added the defect interactions through the Cluster Expansion method but without increasing the solubility considerably. Actually, our formalism includes the solute-solvent ordering tendency by considering the real intermetallic ground state other than the pure Ti-solid. Thus, we conclude that our approximations (or those of the cluster expansion method) are not responsible for the theory-experiment solubility discrepancy.

In case of Ti-Zn, the formation enthalpy is very low (see Table II). Correspondingly, the theoretically solu-

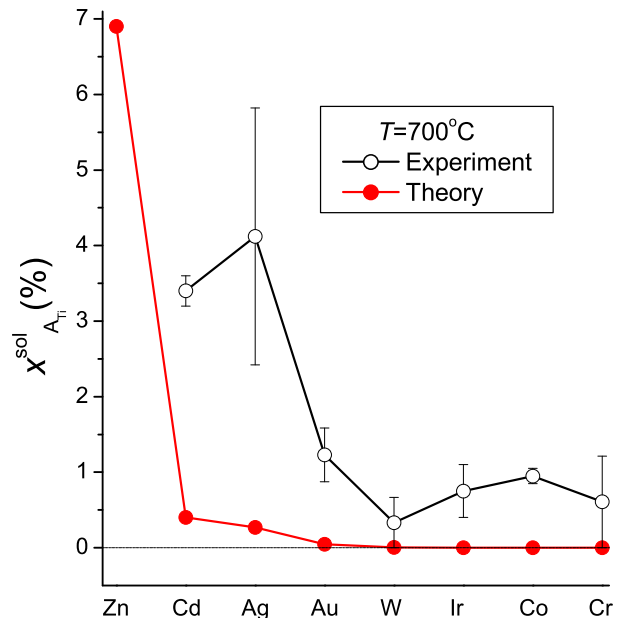


FIG. 12: (Color online) Comparison of experimental[36, 37] and theoretical solubilities of eight considered transition metals in titanium at $T=700^{\circ}\text{C}$. From left to right, the elements are ordered from low to high low-solubility formation enthalpy (and correspondingly theoretical solubility) The error bars characterize the scattering of data measured in different experiments. We could not find the experimental data for solubilities in Ti-Zn.

bility at intermediate temperatures is very high, violating the assumptions of the model. Thus, for Zn in Ti, a more precise solute interaction and correlation parameterizations is required, which can be obtained by using, for example, Cluster Expansion and Monte Carlo simulations. Hence, the presented formalism should be considered as an appropriate starting point to determine if more computationally expensive formalisms are needed.

The other approximation of our model is the assumed independence of our model energy and volume parameters on temperature. The dependence can be caused by non configurational degrees of freedom, like vibrational or anharmonicity (magnetic ordering is not actual for considered alloys). However, theory-experiment solubility discrepancy is observed even at low enough temperatures (e.g. $T \leq \Theta_{\text{p}}(\text{Ti}) = 374\text{-}385\text{ K}$ [41]), where the vibrational contribution to the free energy is not important. In fact, vibrational entropy is substantially smaller than the configurational contribution [42], so its inclusion can not modify solubility results much. In fact, even in Ref. 21, the authors added phonon contribution without increasing the solubility considerably.

On the other side, the experimental equilibrium solubility tends usually to be overestimated. In fact, the formation of metastable and/or unstable states which are subsequently frozen at low temperatures, can make solu-

bility measurements very challenging. In such scenarios, the measured solubility may correspond to spinodal concentration rather than actual binodal concentration or simply characterize the frozen out of equilibrium solubility remaining from the initial specimen preparation at higher temperature. Besides, the segregation of defects into grain-boundaries, especially in multicrystalline samples prepared through non optimal cooling dramatically affect the amount of frozen defects and solutes.

VI. CONCLUSIONS

Based on the statistical-thermodynamic theory of dilute lattice gas, we developed an approach to calculate the atomic bulk solubility in alloys. The advantage of our approach consists in considering all the appropriate ground states rather than the pure species. It was shown that the low-solubility follows simple Arrhenius-type temperature dependence determined by a “*low-solubility formation enthalpy*”. This quantity is defined as the composition derivative of the compound formation enthalpy with respect to nearby ground states. “Low-solubility formation enthalpy” coincides with the usual defect formation enthalpy only in the case of a phase-separating alloy having no intermediate ground states and vacancies. The key quantities of our model can be directly obtained

by first-principles calculations or by fitting experimental temperature solubility dependence. Generalization of our model to intermediate phases and/or to multicomponent, multisublattice, interstitial-substitutional alloys is straightforward.

As examples, we applied the framework for a set of eight Ti alloys A-Ti (A=Ag,Au,Cd,Co,Cr,Ir,W,Zn). We have found that the highest solubility for Zn, Cd, Ag, and Au is in qualitative agreement with available experimental data and band structure expectations. The quantitative differences between the theory and experiment observed in the present and other similar studies are discussed.

In conclusion, our formalism is correct in the limit of low-solubility and should be considered as an appropriate starting point for determining if more computationally expensive formalisms are otherwise needed.

Acknowledgements

We acknowledge Wahyu Setyawan, Mike Mehl, and Ohad Levy for fruitful discussions. This research was supported by ONR (Grant No. N00014-07-1-0878) and NSF (Grant No. DMR-0639822) We thank the Tera-grid Partnership (Texas Advanced Computing Center, TACC) for computational support (MCA-07S005).

-
- [*] Electronic address: stefano@duke.edu
- [1] Ceder G, Chiang YM, Sadoway DR, Aydinol MK, Jang YI, B. Huang, Nature 1998;392:694.
- [2] Johannesson GH, Bligaard T, Ruban AV, Skriver HL, Jacobsen KW, Nørskov JK, Phys. Rev. Lett. 2002;88:255506.
- [3] Stucke DP, Crespi VH, Nano Lett. 2003;3:1183.
- [4] Curtarolo S, Morgan D, Persson K, Rodgers J, Ceder G, Phys. Rev. Lett. 2003;91:135503.
- [5] Curtarolo S, Morgan D, Ceder G, Calphad 2005;29:163.
- [6] Fischer C, Tibbetts K, Morgan D, Ceder G, Nature Mater. 2006;5:641.
- [7] Hart GL, Blum V, Walorski MJ, Zunger A, Nature Materials 2005;4:391.
- [8] Bligaard T, Johannesson GH, Ruban AV, Skriver HL, Jacobsen KW, Nørskov JK, Appl. Phys. Lett. 2003;83:4527.
- [9] Persson M, Bligaard T, Kustov A, Larsen KE, Greeley J, Johannesson T, Christensen CH, Nørskov JK, J. Catal. 2006;239:501.
- [10] Kolmogorov AN, Curtarolo S, Phys. Rev. B 2006;73:180501(R).
- [11] Calandra M, Kolmogorov AN, Curtarolo S, Phys. Rev. B 2007;75:144506.
- [12] Kolmogorov AN, Calandra M, Curtarolo S, Phys. Rev. B 2008;78:094520.
- [13] Wolverton C, Siegel DJ, Akbarzadeh AR, Ozoliņš V, J. Phys.: Condens. Matter 2008;20:064228.
- [14] Siegel DJ, Wolverton C, Ozoliņš V, Phys. Rev. B 2007;76:134102.
- [15] Akbarzadeh AR, Ozoliņš V, Wolverton C, Advanced Materials 2007;19:3233.
- [16] Cava RJ, Zandbergen HW, Inumaru K, Physica C 2003;385:8.
- [17] Singh RK, Shen Y, Gandikota R, Wright D, Carvalho C, Rowell JM, Newman N, Supercond. Sci. Technol. 2008;21:025012.
- [18] Harutyunyan AR, Awasthi N, Mora E, Tokune T, Jiang A, Setyawan W, Bolton K, Curtarolo S, Phys. Rev. Lett. 2008;100:195502.
- [19] Curtarolo S, Awasthi N, Setyawan W, Jiang A, Bolton K, Harutyunyan AR, Phys. Rev. B 2008;78:054105.
- [20] Sigli C, Maenner L, Sztur C, Shahni R, in Proceedings of the 6th International Conference on Aluminum Alloys (ICAA-6), edited by T. Sato et al. (Japan Institute of Light Metals, 1998), Vol. 1, p. 87
- [21] Clouet E, Sanchez JM, Sigli C, Phys. Rev. B 2002;65:094105.
- [22] de Fontaine D, in *Solid State Physics*, edited by H. Ehrenreich and D. Turnbull (Academic Press, New York, 1994), Vol. 47, pp. 33176.
- [23] Ceder G, Comput. Mater. Sci. 1993;1:144.
- [24] Xu Q, Van der Ven A, Phys. Rev. B 2007;76:064207.
- [25] Van der Ven A, Ceder G, Phys. Rev. B 2005;71:054102.
- [26] Wagner C, Schottky W, Z. Physik. Chem. B 1930;11:163.

- [27] Mishin Y, Farkas D, Phil. Mag. A 1997;75:169. Y. Mishin C. Herzig, Acta Mater. 2000;48:589.
- [28] Korzhavyi PA, Ruban AV, Lozovoi AY, Vekilov YK, Abrikosov IA, Johansson B, Phys. Rev. B 2000;61:6003.
- [29] Matysina ZA, Milyan MI, Zaginaichenko SY, J. Phys. Chem. Solids 1988;49:737.
- [30] The existence of such unknown ground state was predicted upon Be substitution of Mg in MgB₇ in Chepur-skii RV, Mazin II, Curtarolo S, *First-principles search for potential high temperature superconductors in the Mg-B-A (A=alkali and alkaline earth metals) system with high boron content*, submitted (2009).
- [31] Kresse G, Hafner J, Phys. Rev. B 1993;47:558.
- [32] Blochl PE, Phys. Rev. B 1994;50:17953.
- [33] Perdew JP, Burke K, Ernzerhof M, Phys. Rev. Lett. 1996;77:3865.
- [34] So that by calling enthalpy we actually mean energy in this section.
- [35] Curtarolo S, *Aflow: a computational software to calculate properties of materials in a high-throughput fashion*. <http://materials.pratt.duke.edu/afLOW.html>
- [36] Villars P, Cenzual K, Daams JLC, Hulliger F, Massalski TB, Okamoto H, Osaki K, Prince A, Iwata S, Crystal Impact, *Pauling File. Inorganic Materials Database and Design System*, Binaries Edition, ASM International, Metal Park, OH (2003)
- [37] *Binary Alloy Phase Diagrams*, edited by T. B. Massalski (ASM International, Metals Park, OH, 1992)
- [38] *International Tables for Crystallography*, Vol. A, edited by T. Hahn (D. Reidel, Dordrecht, 1983).
- [39] J. Friedel, in *Physics of Metals*, edited by J. M. Ziman (Cambridge University Press, Cambridge, 1969), p. 495.
- [40] Krivoglaz MA, Smirnov AA, *The Theory of Order-Disorder in Alloys* (Macdonald, London, 1964).
- [41] Chen Q, Sundman B, Acta Mater. 2001;49:947.
- [42] van de Walle A, Ceder G, Rev. Mod. Phys. 2002;74:11.